The Efficient Separation of N_2O/CO_2 using Unsaturated Fe^{2+} Site in MIL-100Fe

Li Wang[a], Feifei Zhang [a], Jiangfeng Yang[ab]*, Libo Li[ab], Jinping Li[ab]*

[a] Research Institute of Special Chemicals, College of Chemistry and Chemical Engineering, Taiyuan University of Technology, Taiyuan 030024, Shanxi, P. R. China.

[b] Shanxi Key Laboratory of Gas Energy Efficient and Clean Utilization, Taiyuan 030024, Shanxi, P. R. China.

Supporting Information

1. Materials

The commercially available reagent grade chemicals were used as received without any further purification. Metal iron powder (Fe, Aladdin, 99%), 1,3,5-benzenetricarboxylic acid or trimesic acid (H_3BTC, Aladdin, 98%), hydrofluoric acid (HF, 40%, Sinopharm Chemical Reagent Co., Ltd.), nitric acid (HNO_3, 63%, Tianjin Yaohua Chemical Reagent Co., Ltd), ethanol (CH_3CH_2OH, AR, Sinopharm Chemical Reagent Co., Ltd.), deionized water (H_2O, homemade).

MIL-100(Fe) was prepared in our lab via a literature reported method and with some modifications.[1] Metal iron powder (10 mmol, 0.56g) and trimesic acid (6.7 mmol, 1.41g) are added in the water (50 ml), and then 0.90 ml HF and 0.42 ml HNO_3 are added to the above solution. The reactant mixture was loaded in a Teflon autoclave. The autoclave was heated up to reaction temperature and kept at 150°C for 12 h. The pH remains acidic throughout the synthesis. The light orange solid product was recovered by filtration, washed with deionized water. The as synthesized MIL-100(Fe) was further purified by two-step processes using hot water and ethanol. The purification has been performed using boiling water at 80°C for 5 h to decrease the amount of residual unreacted ions (typically, 1 g of MIL-100(Fe) in 350 ml of water) and then hot ethanol at 60℃ for 3 h until no detection of colored impurities in the mother liquor solution, resulting in the highly purified MIL-100(Fe). The solid was finally dried overnight less than 100°C under nitrogen atmosphere.

2. Characterization

The powder X-ray diffraction (PXRD) patterns were recorded on a Bruker D8ADVANCE powder X-ray diffractometer equipped with Cu Kα radiation in the 2θ ranges from 2° to 20° at 40 kV and 40 mA. The scanning electron microscopy (SEM) images were recorded in a Hitachi SU8000 microscope. Thermogravimetric analysis (TGA) was carried out under an air atmosphere using a NETZSCH STA 449F5 thermal analyzer at a heating rate of 10°C/min. X-ray photoelectron spectroscopy (XPS) analysis was conducted on ThermoFischer USA，ESCALAB 250Xi with an Al Kα X-ray source (hv=1486.6 Ev) operating at 12.5 Kv and 16 mA. The vacuum of the analysis chamber is 8×10^{-10} Pa and carry out 10 cycles of signal accumulation. The full spectrum of passing energy is 50 ev, the narrow spectrum is 20 ev, the step size is 0.05 ev, and the residence time is 40-50 ms. The charge correction was carried out with the binding energy of C1s = 284.80 ev as the energy standard. The infrared spectrum was measured by Shimadzu FT-IR 8400 s Fourier transform infrared spectrometer, and the sample was dried in an oven at 353 K for 2 h before the test. The infrared spectrum was measured by Bruker v70 Fourier transform infrared spectrometer (FTIR), and the sample was dried in an oven at 353 K for 2 h before the test.

3. Adsorption isotherms measurement

N_2 adsorption–desorption isotherms were measured on ASAP 2020 apparatus at 77 K. The N_2O and CO_2 adsorption isotherms were measured on ASAP 2460. For each test, ~50 mg of the MOFs sample was loaded and outgassed prior to the gas sorption measurements. All the gases used (CO_2, N_2O, N_2 and He) were of 99.99% purity.

Before the gas sorption studies, MIL-100Fe was activated in the activation station for about 12 h under different temperature (150 ℃-350 ℃). The sample in the powder form was characterized by powder X-ray diffraction (PXRD), thermal gravimetric analysis (TGA), N_2 adsorption-desorption isotherms at 77 K, and X-ray photoelectron spectroscopy (XPS) analysis.

4. Fitting of pure component isotherms

In order to properly capture the isotherm inflections, the unary isotherm data of CO_2 and N_2O were fitted with the Langmuir-Freundlich model:

$$q = q_{sat} \frac{bp^{v}}{1 + bp^{v}} \quad (1)$$

The saturation capacities q_{sat}, Langmuir constants b, and the Freundlich exponents ν, for CO_2 and N_2O are provided in supporting information.

5. Ideal adsorbed solution theory (IAST) gas selectivity of N_2O/CO_2

In order to check the N_2O/CO_2 separation ability of MIL-100Fe, IAST calculations of N_2O/CO_2 (50%/50%) mixture adsorption were performed based on the single gas adsorption isotherm. The adsorption selectivity and separation ability of MIL-100Fe toward N_2O/CO_2 mixture were evaluated based on the IAST calculations.

The IAST calculation was then used to estimate the selectivity of a 50%:50% (v:v) N_2O/CO_2 gas mixture. The adsorption selectivity was calculated from

$$S_{ads} = \frac{q_1/q_2}{p_1/p_2} \quad (2)$$

In equation (2), q_1 and q_2 are the molar loadings in the adsorbed phase in equilibrium with the bulk gas phase with partial pressures p_1 and p_2.

6. Isosteric heats of adsorption

The isosteric heats of adsorption (Q_{st}) values were calculated from isotherms measured at 273 K and 298 K for N_2O and CO_2. The isotherms were fit to a viral equation (3).

$$ln\, P = ln\, N + \frac{1}{T}\sum_{i=o}^{m} a_i N^i \; + \sum_{i=o}^{n} b_i N^i \quad (3)$$

Where N is the amount of gas adsorbed at pressure P, a and b are virial coefficients, m and n are the numbers of coefficients require to adequately describe the isotherm. Using the fitting parameters obtained from the above equation, Q_{st} can be calculated using the following Eq. (4).

$$Q_{st} =- R\sum_{i=o}^{m} a_i N^i \qquad (4)$$

R is the universal gas constant.

7. DFT calculation

The DFT calculations are performed by the CASTEP package codes.[2] The density functional was performed by the generalized gradient approximation (GGA) with the Perdew-Burke-Ernzerhof (PBE) exchange-correlation functional,[3] as well as the DFT-D was adopted to describe the Van der Waals interaction. The k-point was set as 2×2×2 for the graphene related slabs and the cuto□ energy was set as 580 eV, the self-consistent field (SCF) convergence criterion of 1×10^{-6} eV/atom was adopted to the geometry optimization and electronic computations. The binding energies (E_b) was calculated as $E_b= E_{M+X} - E_M - E_X$, where the E_{M+X} is the total energy of the MOF core cluster adsorbed with the CO_2 or N_2O, E_M is the energy of the MOF core cluster, as well as the E_x is the energy of free CO_2 or N_2O.

8. Breakthrough separation experiments and procedures

The experimental setup consists of three parts: gas flow, adsorption bed and mass spectrometry (MS, HPR-20, Hiden).[4] The adsorption bed was a stainless-steel column (inner diameter: 4mm, 100 mm). In the experiment, we packed MIL-100Fe-150 and MIL-100Fe-300 powder into a stainless-steel column. At the same time, the adsorption bed was purged with a carrier gas (He ≥ 99.999%) at a rate of 20 mL/min. However, for N_2O/CO_2 mixtures, which have the same relative molecular mass, the intense m/e = 44 peaks overlap, and thus, we chose pieces of the m/e (CO_2) = 12.00 and m/e (N_2O) = 30.00 peaks to separate CO_2 and N_2O.

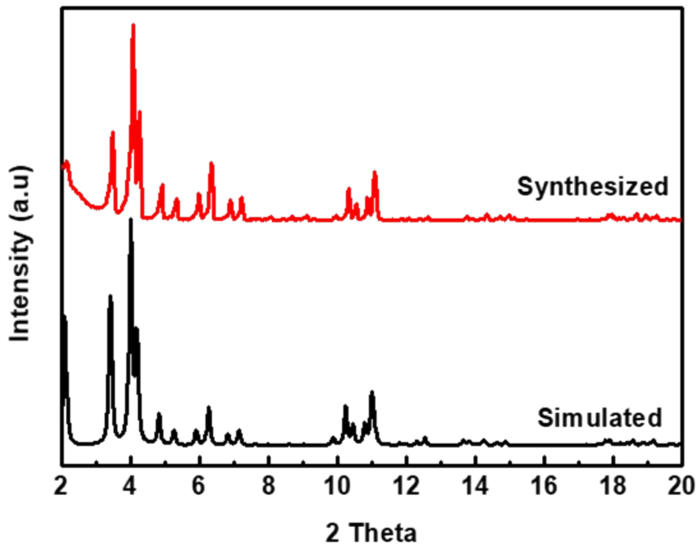

Figure S1 PXRD patterns of MIL-100Fe.

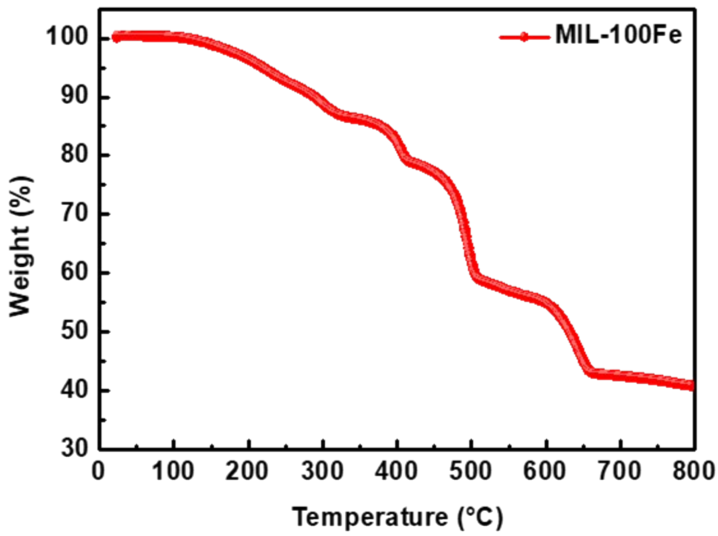

Figure S2 TGA curve of MIL-100Fe.

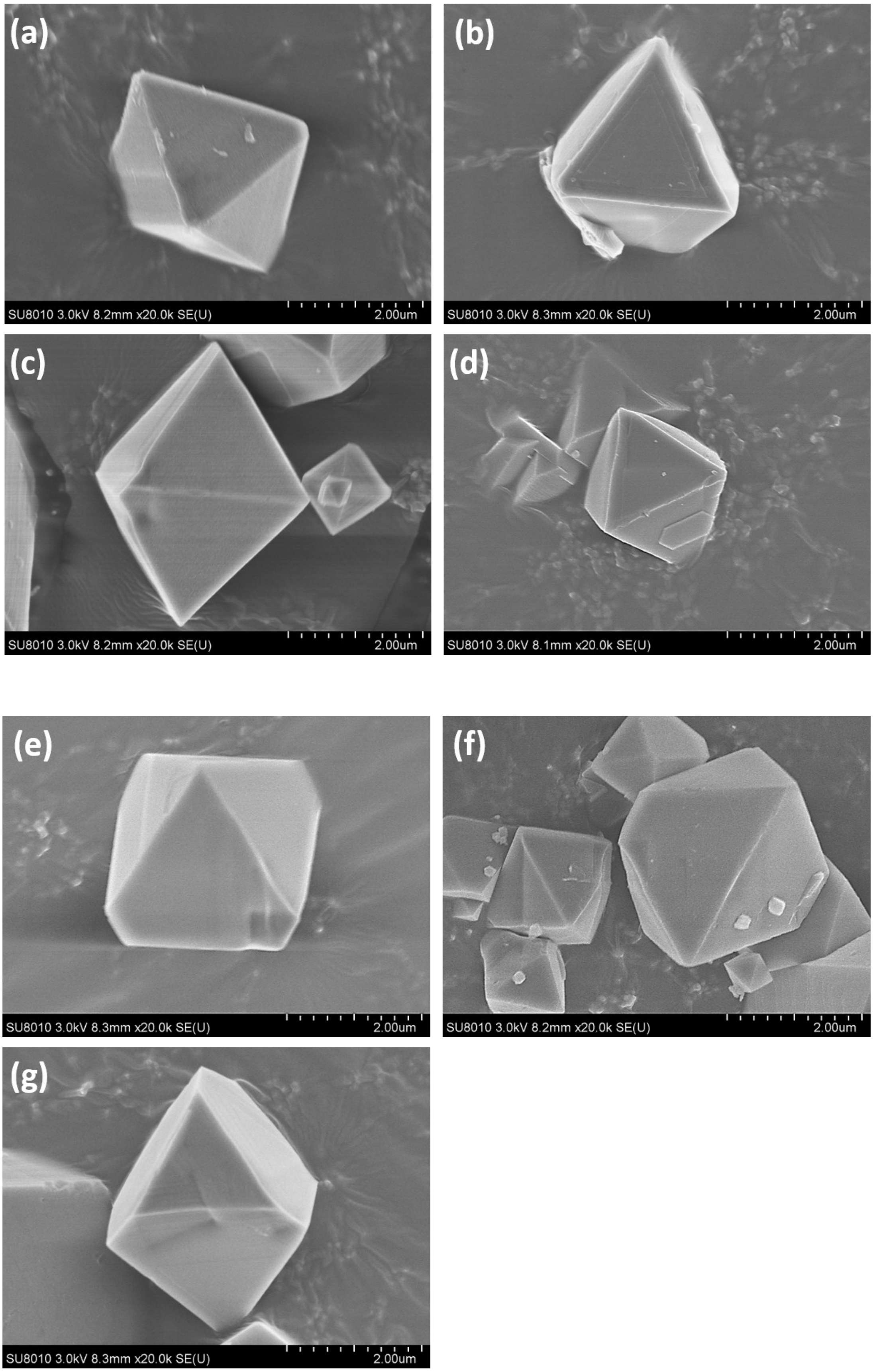

Figure S3 SEM image of MIL-100Fe synthesized (a) and after 150 ℃ (b), 200 ℃ (c), 250 ℃ (d), 290 ℃ (e), 300 ℃ (f) and 310 ℃ (g) activated.

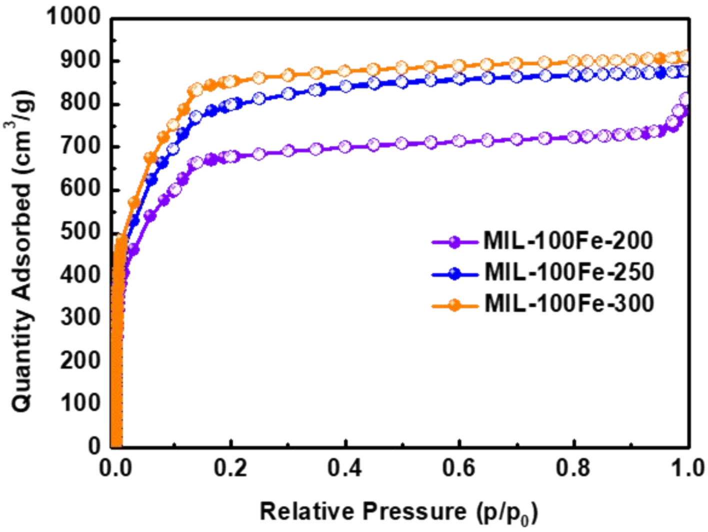

Figure S4 77 K N_2 adsorption-desorption isotherms of MIL-100Fe after different temperature activated.

Table S1 BET surface area and pore volume of MIL-100Fe after different temperature activated.

Sample	MIL-100Fe-200	MIL-100Fe-250	MIL-100Fe-300
BET surface area (m^2/g)	2006.12	2159.68	2227.00
Pore volume (cm^3/g)	1.25	1.35	1.40

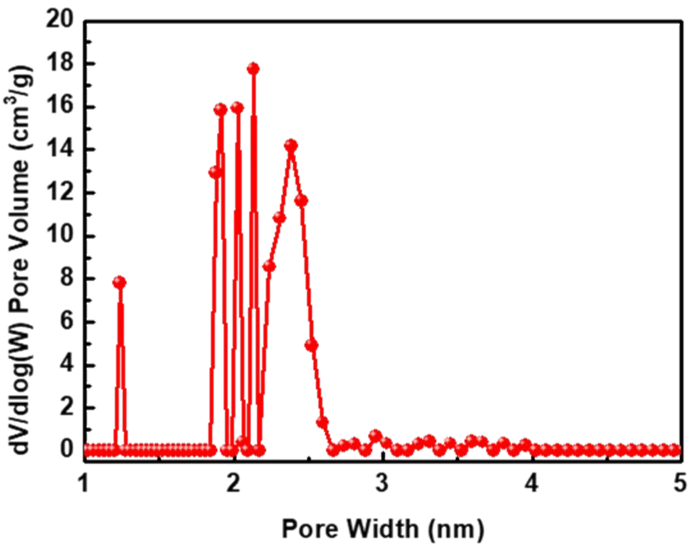

Figure S5 77 K N_2 adsorption-desorption isotherms and the pore size distribution calculated by the DFT method.

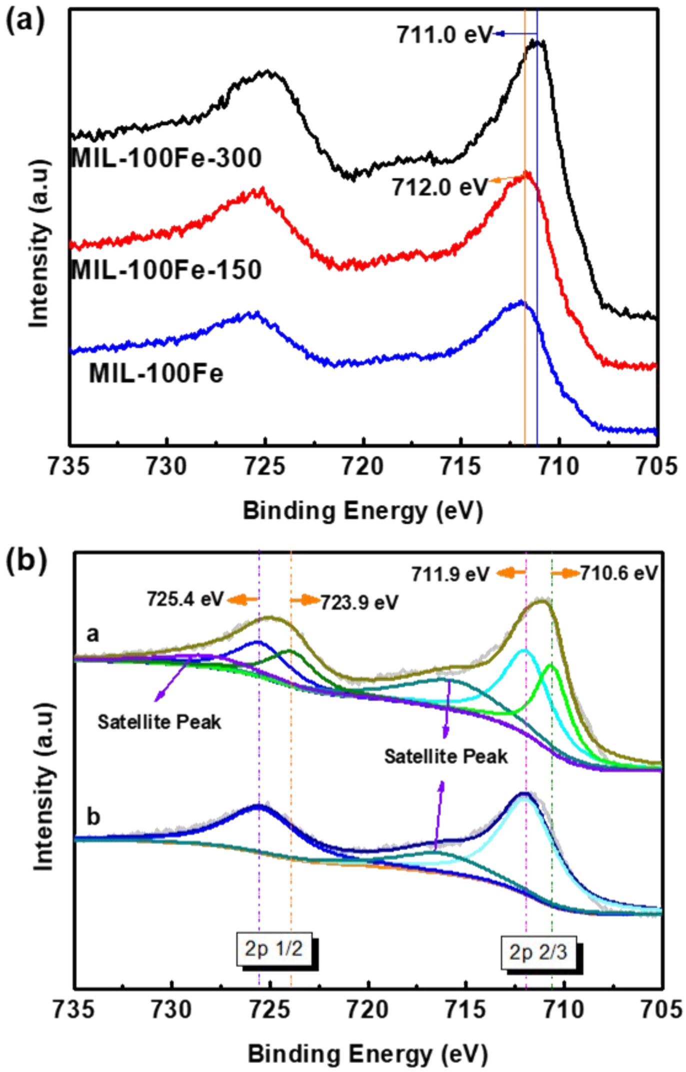

Figure S6 High-resolution XPS spectra of Fe 2p for the comparison of MIL-100Fe, MIL-100Fe-150 and MIL-100Fe-300 (a) and the detail of MIL-100Fe-300 and MIL-100Fe (b).

Table S2 Atomic content of F, Fe and F/Fe ratio at different activation temperatures.

Sample	F (atom %)	Fe (atom %)	F/Fe
MIL-100Fe-150	2.07	7.83	0.2644
MIL-100Fe-200	1.66	7.59	0.2187
MIL-100Fe-250	1.27	8.82	0.1440
MIL-100Fe-300	0.63	8.7	0.0724

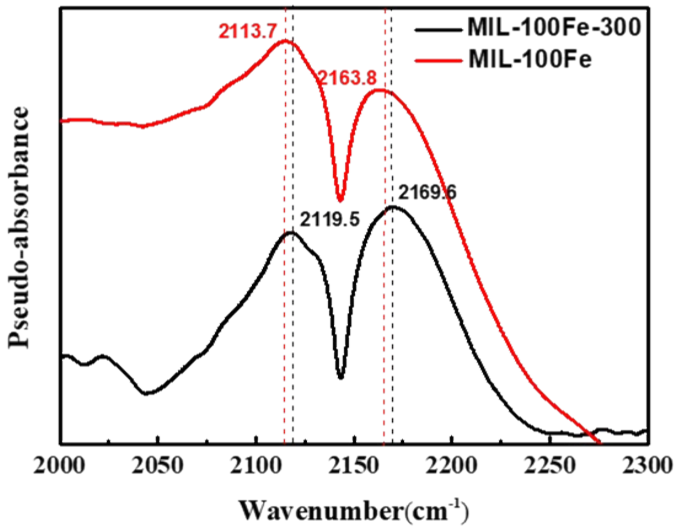

Figure S7 FTIR of MIL-100Fe and MIL-100Fe-300 under a steam of 10% CO at 25 ℃ after activation under vacuum condition

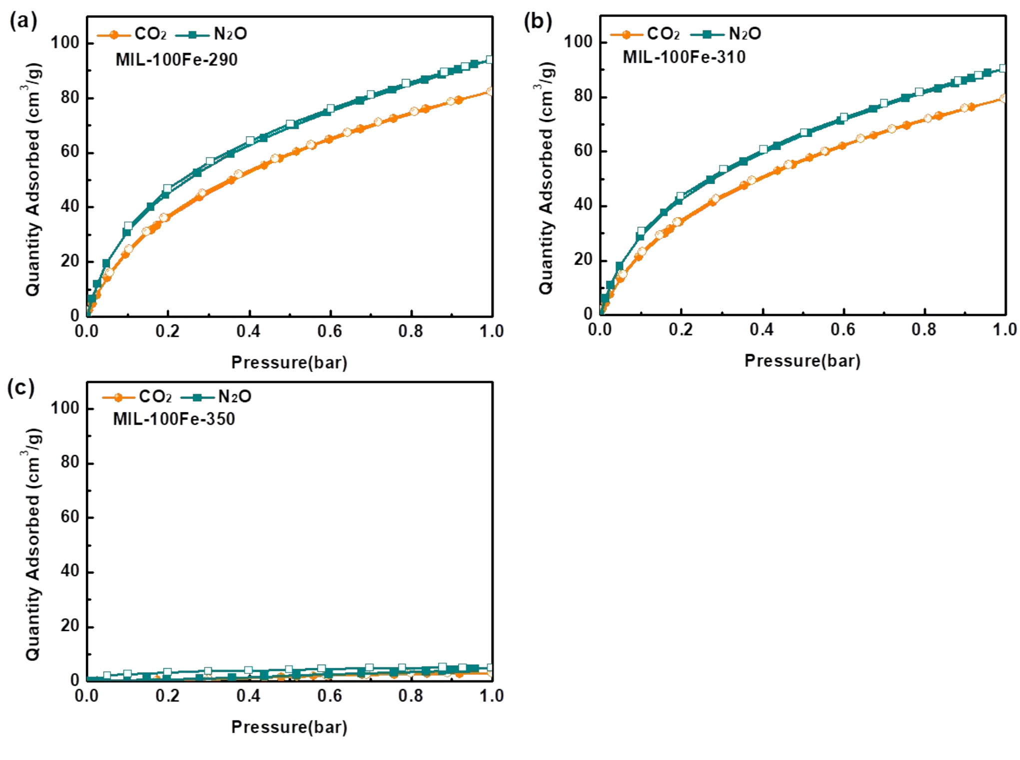

Figure S8 Adsorption isotherms of CO_2 and N_2O at 298 K on MIL-100Fe-290 (a), MIL-100Fe-310 (b) and MIL-100Fe-350 (c).

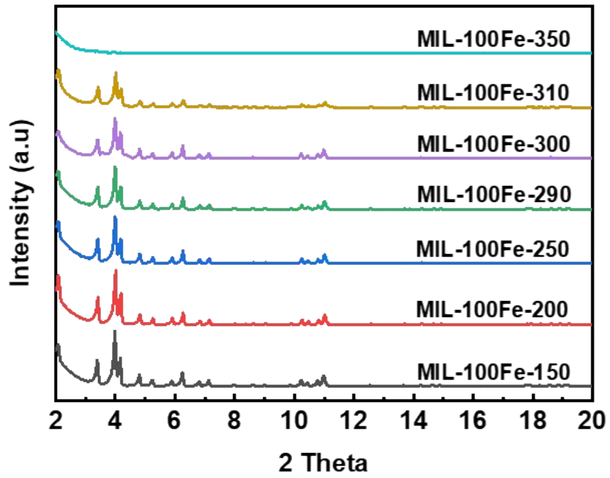

Figure S9 PXRD patterns of MIL-100Fe after different temperature activated.

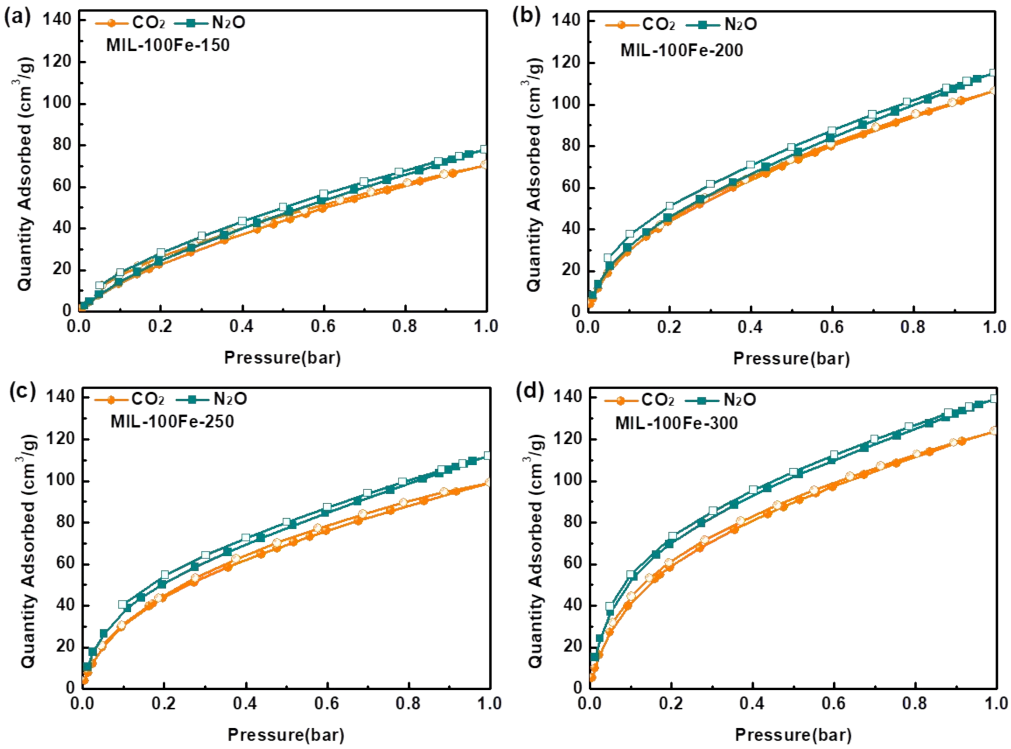

Figure S10 Adsorption isotherms of N_2O and CO_2 at 273 K after different activation temperature (a) 150 ℃ (b) 200 ℃ (c) 250 ℃ (d) 300 ℃

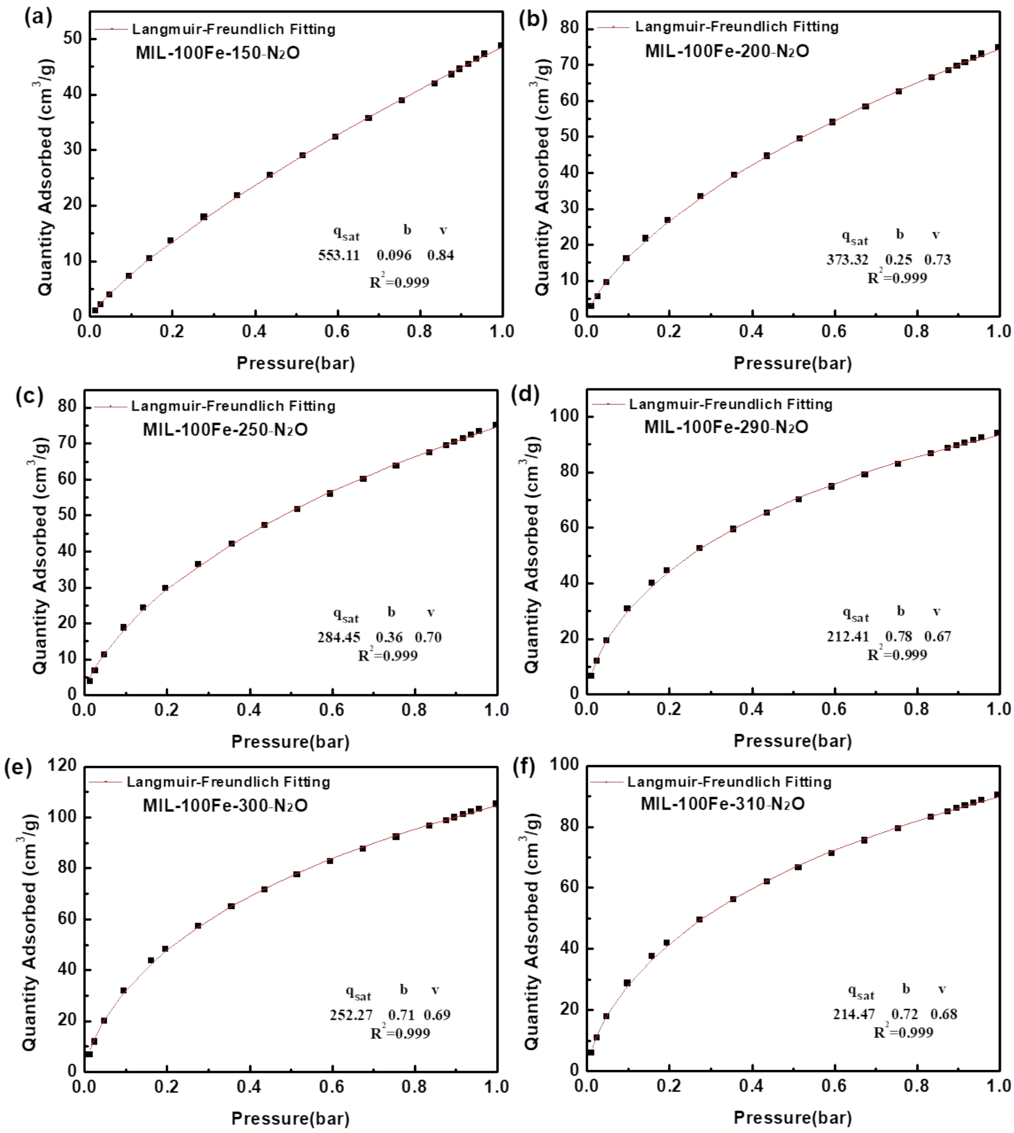

Figure S11 Langmuir-Freundlich Fitting curves of N_2O adsorption isotherms at different activated temperature and 298 K

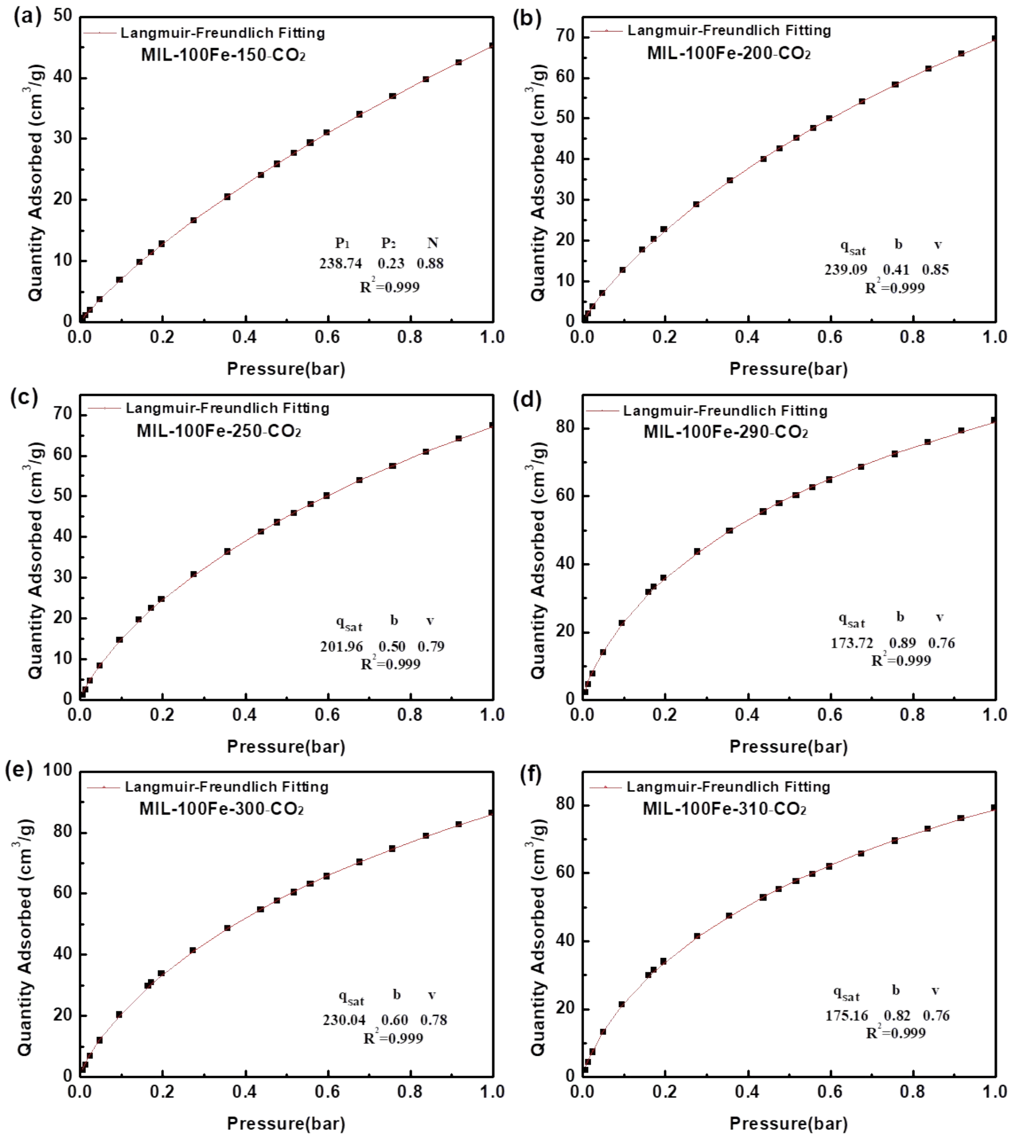

Figure S12 Langmuir-Freundlich Fitting curves of CO_2 adsorption isotherms at different activated temperature and 298 K.

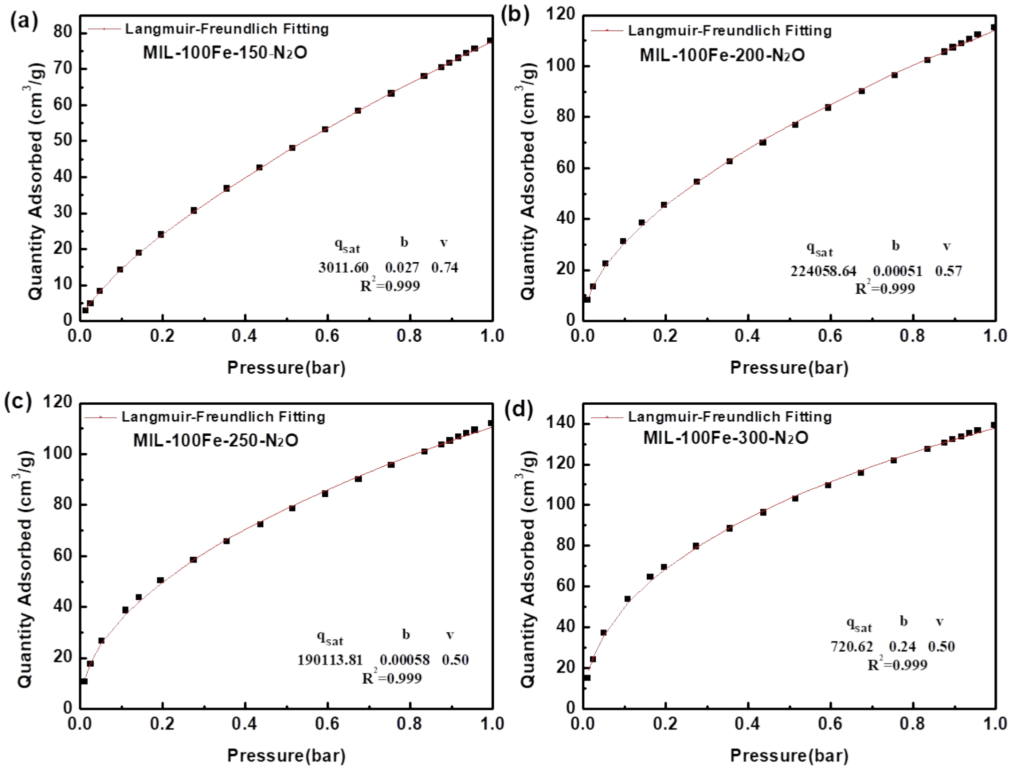

Figure S13 Langmuir-Freundlich Fitting curves of N_2O adsorption isotherms at different activated temperature and 273 K.

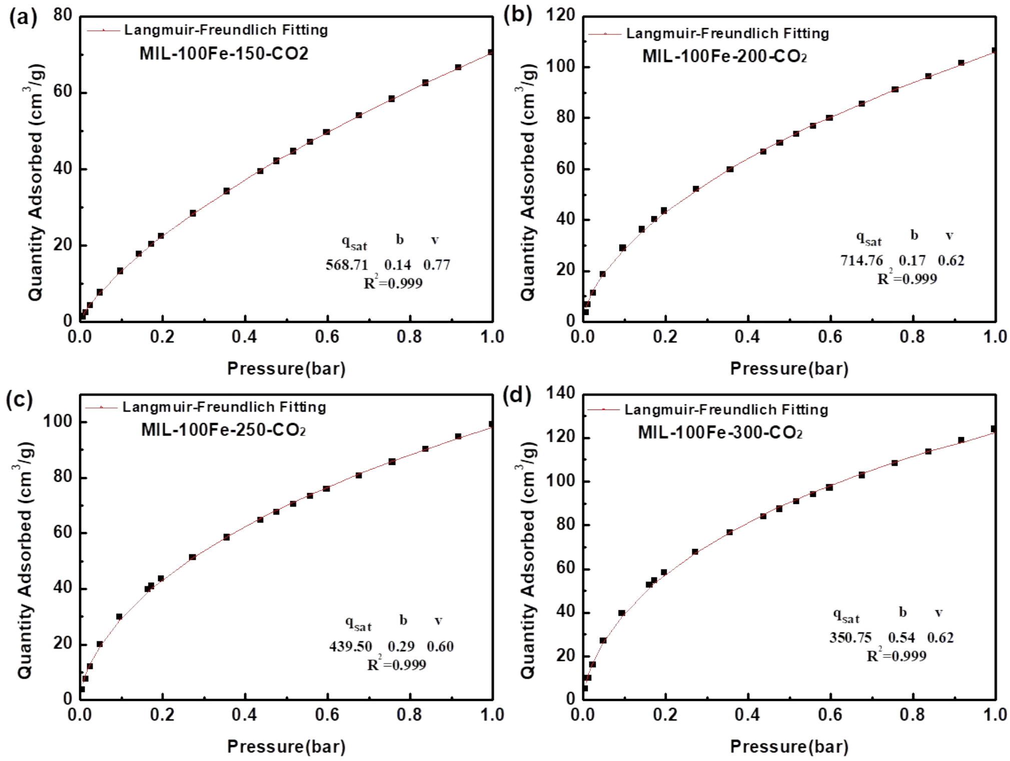

Figure S14 Langmuir-Freundlich Fitting curves of CO_2 adsorption isotherms at different activated temperature and 273 K.

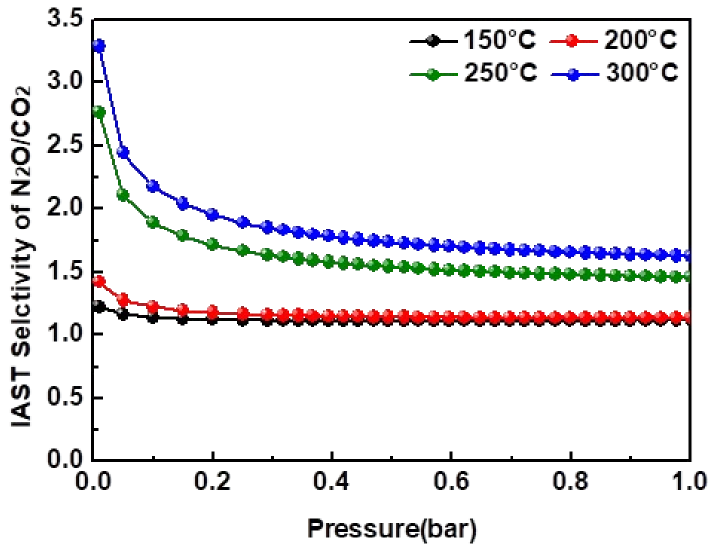

Figure S15 IAST selectivity of 50%/50% N_2O/CO_2 at 273 K.

Table S3 Adsorption capacity of N_2O and CO_2 and N_2O/CO_2 selectivity on MIL-100Fe-X at 298 K and 1 bar.

Sample	N_2O uptake (cm^3/g)	CO_2 uptake (cm^3/g)	IAST Selectivity of N_2O/CO_2	Ref.
MIL-100Fe-200	74.98	69.50	1.27	This work
MIL-100Fe-250	75.10	67.40	1.35	This work
MIL-100Fe-290	94.06	82.41	1.54	This work
MIL-100Fe-310	90.34	79.40	1.51	This work
MIL-100Fe-350	4.95	3.03	-	This work

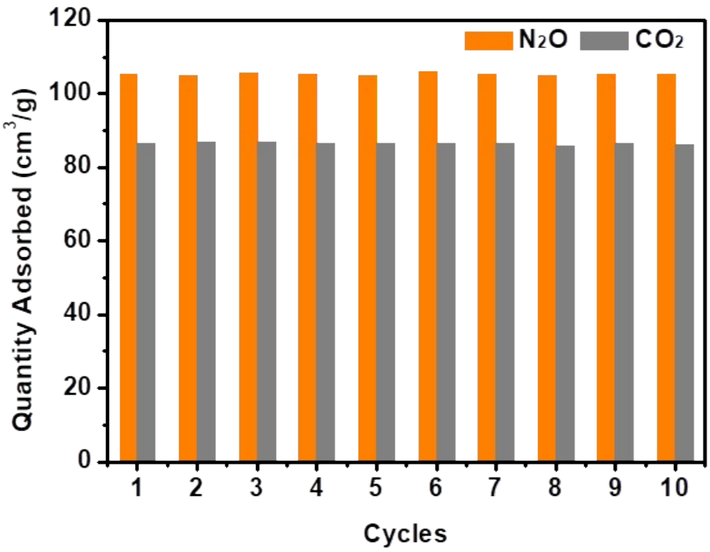

Figure S16 CO_2 and N_2O adsorption-desorption recycles on MIL-100Fe-300.

References

1. J. W. Yoon, Y.-K. Seo, Y. K. Hwang, J.-S. Chang, H. Leclerc, S. Wuttke, P. Bazin, A. Vimont, M. Daturi, E. Bloch, P. L. Llewellyn, C. Serre, P. Horcajada, J.-M. Grenèche, A. E. Rodrigues and G. Férey, *Angew. Chem. Int. Edit.*, 2010, **49**, 5949-5952.
2. S. J. Clark, M.D. Segall, C.J. Pickard, P.J. Hasnip, M.I.J. Probert, K. Refson, M.C. Payne, Z. Krist., 2005, **220**, 567-570.
3. J. P. Perdew, K. Burke, M. Ernzerhof, *Phys. Rev. Lett.*, 1996, **77**, 3865-3868.
4. L. Wang, Y. Li, Y. Wang, J. Yang, L. Li and J. Li, *Sep. Purif. Technol.*, 2020, **251**,117311.